

THE ROLE OF SYNTHESIS PHENYL-ETHANOL DI-TRIETHANOL
AMINE SILOXANE COMPOUND IN THE FORMATION OF
POLYURETHANE PROTECTIVE COATINGS ON CARBON STEEL

O. M. Abo-Elenien, M. A. Abbas; M. A. Elsoukary; and H.M. Abd Elbary*
Egyptian Petroleum Research Institute (EPRI), Ahmed El-Zomor St., 1, Nasr City
11727, Cairo, Egypt

*Chemistry Department, Faculty of Science, Al- Azhar University, Nasr City, Cairo,
Egypt

Received:(2/11/2011)

ABSTRACT

The new organosilicon compound was prepared and confirmed by IR, ¹HNMR, GLC, GPC and elemental analysis. This compound was formulated with other organic (furan, epoxy and novolac) and inorganic (zinc dust, calcium carbonate, talc, sintered glass and titanium oxide) to form some formulas. These formulas were applied on the carbon steel specimens. The toluene diisocyanate (TDI) was used as curing agent at different ratios. The optimum conditions were studied; the physical, mechanical, electrochemical properties for dry film formed on the carbon steel surface were investigated. Finally the surface morphology for dry films was studied before and after electrochemical tests.

Keywords: Painted carbon steel; Impedance measurements; Equivalent circuits, organic coatings, surface properties, cyclic voltammetry, EIS, SEM.

INTRODUCTION

The advantages of combining organic and inorganic components have been frequently described for organic-inorganic hybrid materials, in which these components are mixed at the molecular level. Applications of organic-inorganic materials in many fields, such as protective coatings [Yeh JM, (2006) and Aparicio M, (2006)] were studied. The introduction of an inorganic component in an organic matrix has been used, for instance, to improve the selectivity of hydrocarbons in silicone membranes [Nunes SP, (1996)]. Organic coatings may be used to protect metallic materials against aggressive environments. Generally, inhibitive pigments are introduced into organic coatings as the main substance for corrosion inhibition. For this purpose, zinc phosphate is commonly used because it is known as a green pigment in contrary to toxic pigments like chromate pigments [Benbachir, A. *et al* (1999), Ashirgade, A *et al* (2007), Deya, M.C. *et al* (2002), Mahdavian, M. *et al* (2005), Zubielewicz, M. *et al* (2004), Sinko, J.

et al (2001), Bethencourt, M. *et al* (2003), and Chromy, L. *et al* (1990)]. Epoxy is one of the most common coating materials used in severe corrosion environments including marine environment [May, C.A. (1988), and Goulding, T.M. (1994)]. Due to the hydrophilic chemical groups of cured epoxy structure such as hydroxyl group (-OH), carboxyl group (COO) and amino group (Aronhime, M.T. *et al* (1986), Zhou, J.M *et al* (1999),) that have unpaired electron, epoxy has exhibited the hydrophilic properties by attracting water from the environment [Nunez, L. *et al*, (1999), Xiao, G.Z. (1997) *et al* and Lezzi, R.A. *et al* (1997)] to which it is exposed, resulting in a decrease in its protectiveness for metal underneath. Accordingly, there have been a lot of efforts to improve the protectiveness of epoxy coats, considering their material cost and applications, etc. Hydrophobic coating materials such as fluorine [Shon, M. *et al* (2007)] and silicon polymer were introduced for special purposes requiring high corrosion protection, especially as a top coating in heavy duty environments or an anti-fouling coating in shipbuilding industry. However, the applications of these polymers have been limited due to their bad workability during painting work, poor adhesion and expensive material cost. A blending technology combining hydrophilic polymer with hydrophobic polymer may produce an attractive coating system having both high corrosion protection and good adhesion. [Cabanelas, J.C. *et al* (2001), Gonzalez, M. *et al* (2004), Cabanelas, J.C. *et al* (2003), McIntyre, J.M. (1996) and Gonzalez, S. *et al* (2001)]. Electrochemical impedance spectroscopy (EIS) is a well-known electrochemical means to evaluate the performance of organic coatings, and has proven to be a powerful tool for acquiring specific parameters of systems of organic coatings/metals, therewith providing very useful kinetic and mechanism information [Marchebois, H. *et al* (2002), and Zhang, J.T. *et al* (2004)]. In this work, a new compound was synthesized and confirmed by IR, ¹HNMR, GLC, GPC and elemental analysis. This compound was blended with furan, novolac, epoxy, toluene diisocyanate, talc, calcium carbonate, sintered glass, Zn dust, titanium dioxide and butanone as the solvent to form different formulas. These formulas were applied on the preparation carbon steel surface. The physical, mechanical, and electrochemical properties of dry films were investigated. Finally the observed results were indicated that the formed dry films have excellent corrosion protection for carbon steel.

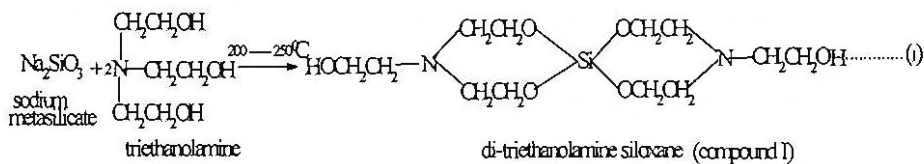
EXPERIMENTAL

1. Materials:

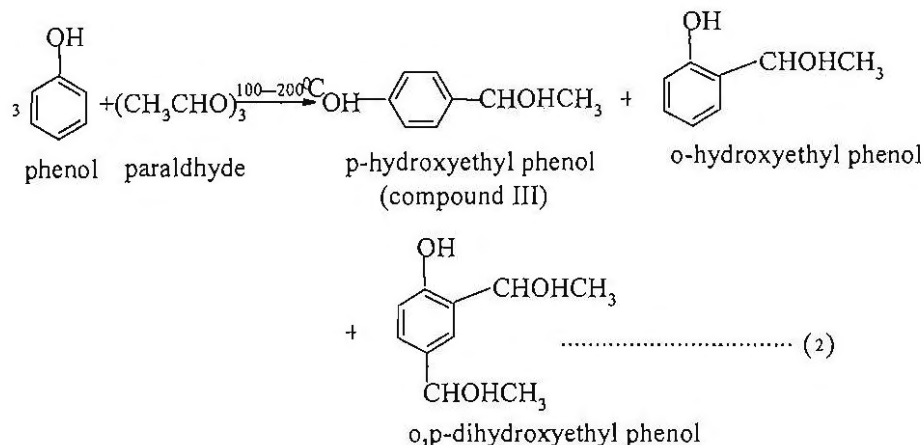
Using chemicals such as: furan, novolac, epoxy, toluene diisocyanate, talc calcium carbonate, sintered glass and Zn dust all were of commercial materials, while sodium metasilicate, ammonium thiocyanate, triethanol amine, titanium dioxide, phenol, paraldehyde and butanone were analytical grade and provided from Alderch.

2. Preparation of the phenyl-ethanol di-triethanol amine siloxane:

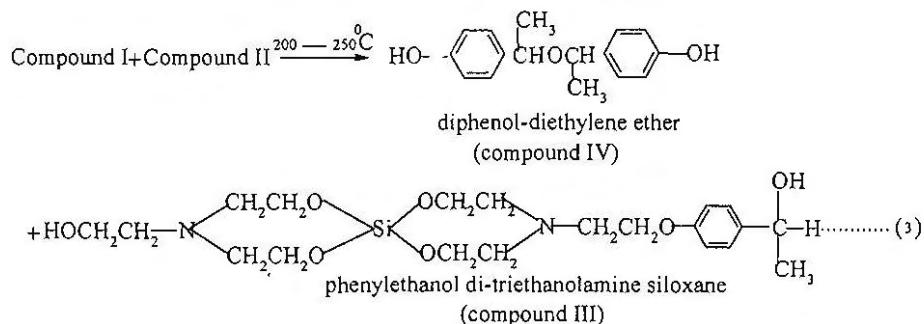
In a three necked round bottom flask, triethanolamine (2 mol) and sodium metasilicate (1 mol) were heated at 120 °C under a N₂ stream with good stirring and maintained for 2 h. The flask was connected to a distillation system and the temperature was rapidly raised to 250 °C and maintained there for 2 h with constant stirring.



Paraldehyde (1 mol) and phenol (3 mol) were heated at 100 °C under a N₂ stream with vigorous stirring and maintained for 2 h, then the temperature was rapidly raised to 200 °C and maintained there for 2 h with constant magnetic stirring.



The product was added to the hot previous mixture from triethanolamine and sodium metasilicate through a funnel and maintained for 2 h with magnetic stirring. Then the reaction mixture was cooled to room temperature and separated by filtration.



Compound III was confirmed by infrared analysis (FT-IR), nuclear magnetic resonance (¹HNMR), gas liquid chromatography (GLC), gas permeation chromatography (GPC) and elemental analysis.

3. Characterization Techniques:

3.1. Infrared Analysis (FT.IR)

The IR spectra of the synthesized compound III were investigated using (FT.IR) Spectrometer Model Type Mattson Bench top 961. The wave number and intensities of the IR of the different types of function groups were determined in the range of 500–4000 cm^{-1} .

3.2. Nuclear Magnetic Resonance (^1H NMR)

The ^1H NMR of the synthesized compound III were determined in dimethyl sulphoxide using 300MHz Spectrometer W-P-300, Bruker.

3.3. Gas Liquid Chromatography (GLC)

The gas liquid chromatography type (Agilent 6890 plus) is used for separation and evaluation the purity of produced compounds.

The conditions for separation were: Detector type: Flame Ionization Detector
Colum: Hp-1 (60m- ID: 0.32mm- DF: 0.5 μm .), Injector temperature: 300 °C, Detector temp.: 320 °C, Initial temperature: 100 °C, Final temperature: 320 °C, Rate separation: 4 °C/min and Carrier: N_2 2 ml/min

3.4. Gas Permeation Chromatography (GPC)

The average molecular weight of compound III was measured by using gas permeation chromatography water model 600E. The conditions for measurement were: Detector type: UV-visible spectrophotometer water, Colum: Styragel columns, Injection volume: 3 μl and Mobile phase: Toluene HPLC grade.

3.5. Elemental Analysis

The elemental analyses of compounds III were carried out at Micro Analytical Center, Faculty of Science - Cairo University, Egypt.

4. Preparation of Formulas (FA10-FA100):

The formulas (FA10-FA100) were prepared by mixing different grams (10 , 20 , 30 , 40 , 50 , 60 , 70 , 80 , 90 , 100) of furan with 10 grams of Novolac, 10 grams of epoxy resin, 10 grams of phenyl-ethanol di-triethanolamine siloxane (compound III) 10 grams of zinc dust, 20 grams of TiO_2 , 20 grams of CaCO_3 , 20 grams of talc, 10 grams of sintered glass and 15 grams of methyl ethyl ketone (MEK) as solvent

5. Evaluation of the Physical and Mechanical Properties:

All measurements were carried out at the environmental conditions (ambient temperature, relative humidity (R.H) at $\approx 50\%$, time of duration for dry film 7 days and dry film thickness 80 ± 5 μm). Films generally are made more visible by use of a magnifier or by use of a pinhole detector.

5.1. Visual Inspection:

The coating films on the surface of specimens were visually inspected to determine sealing, sagging, fish eyes, shrinking, coagulation, smoothes and homogeneity.

5.2. Adhesion Test:

The adhesion of coating film to metallic substrates was carried out by two methods.

(a) An X – cut is made in the film to the substrate, pressure-sensitive tape is applied over the cut and then removed, the adhesion is assessed qualitatively on the (0 – 5) scale.

(b) A lattice pattern with either six cut in two perpendicular directions is made in the film to the substrate, pressure-sensitive tape is applied over the lattice and then removed, the adhesion is evaluated [ASTM (D 3359)].

5.3. Pinhole Test:

The pinhole of the formed films on the surface of carbon steel specimens were measured by Holiday detector model Poro test DC KV 7= 34.3 [ASTM (D-5162)].

5.4. Thermal Cycling Test:

Heats the samples in temperature range gradually from 50 to 325°C increasing by 50°C for approximately 3hr's as a period time for each degree, and then quench it by immersion in water at ambient temperature. The coating is examined for signs of blistering or detachment under a magnification viewer [D-6944-03].

5.5. Bending Test :

This test covers the determination of the resistance to cracking of the formed films on the surface of specimens. It was measured using bending tester 5mm-35mm Richmond Road King stone type KT₂5BQ consisting of a metal cone, a rotating panel- bending arm, and panel clamps all mounted on a metal base. This cone is smooth steel (8 in) in length with a diameter of (1/8 in) at one end and a diameter of (1/2 in) at the other end [ASTM (D-522)].

5.6. Hardness test :

The hardness of the formed film on the specimen's surface was measured using hardness pin test rod model 318. This test was measured at five points, one at the middle of specimen and the others at the four corners [ASTM (D-3363)].

5.7. Impact Test :

The deformations of the formed films on the surface of specimens were determined using Richmond Road, Kingston type KT₂5BQ. Install the punch having the head diameter specified. The test specimen was placed in the apparatus with the coated side up. The specimen is flat against the base support and that the indenter is in contact with the top surface of the specimen. The weight is placed at the zero mark and dropped suddenly on the coated surface of the specimens. The test specimen was removed from the apparatus and the impact area for cracking the coating was estimated. The test repeated five times at each of three heights and the impacted areas are examined by use magnification power [ASTM (D-2794) and (G14-88)].

6. Corrosion studies:

6.1. Salt Spray Test :

Corrosion resistances were tested using the salt spray test according to [ASTM B117]. The electrolyte for this test was 5 % NaCl (by weight) solutions. The corrosion study was carried out in salt spray cabinet (Model: SF/450, Serial No.: CWL/ 87406). After each 500 h exposure period, the panels were rinsed and visually examined for the presence of any corrosion, blistering, softening, staining or other film defects and repositioned in the exposure cabinet to ensure uniformity of exposure conditions. The panel were exposed for a total of 1000 h and examined again.

6.3. Electrochemical Technique

6.3.1. Electrochemical Polarization

The electrochemical polarization and cyclic voltametry effect on the formed films using formulas (FA10-FA100) were measured by Potentiodynamic Polarization Radiometer Voltalab master potentiostat model Voltalab Master 40 Type GZ 301. The coated and uncoated specimens were used as working electrode and measured with respect to saturated calomel electrode (SCE) as the reference electrode and the counter electrode is platinum in 3.5% NaCl solution. The measurements were carried out at scan rate 2.5 mVs⁻¹ and potential range from -1000 to -250 mV/SEC and -1000 to +1000 mV/SEC in the synthesized seawater, respectively.

6.3.2. Electrochemical Impedance (EIS)

A Radiometer Voltalab Master 40 Type GZ 301 Fitting with analysis program Zsimpwin was used for measuring the electrochemical impedance in a wide frequency range from 100 kHz to 1mHz with ± 10 mV and 10 points per decades in the synthesized sea water.

7. Surface Morphology:

The surface morphology for the formulation dry films using the formula (FA90) on the surface of carbon steel specimen was measured by A Jeol (840X Japan) scanning electron microscope (SEM) equipped with an Olympus Camera before and after electrochemical tests.

RESULTS AND DISCUSSION

1. Characterization Techniques:

1.1. Infrared Analysis (FT.IR)

Figure (1) declared that the two bands appeared at 1071 and 1032 cm⁻¹ were corresponded to the stretching mode of Si-alkoxy group. The band appeared at 1151 cm⁻¹ was the —C—O—C group. The presence of three bands in the vicinity of 2946, 2880 and 1403 cm⁻¹ were assigned to stretching vibrations of the asymmetric and symmetric —CH₂— groups, respectively. The bands at 2364 and 2338 cm⁻¹ were assigned to —CH₂—methyl group. The band appeared at 3348 cm⁻¹ was shown the stretching mode of —OH

group. The bands at 881, 755 and 691 cm^{-1} were assigned to the stretching vibrations of para and ortho substituted. The bands at 1650 and 1587 cm^{-1} were assigned to stretching vibration C=C for aromatic ring. The two bands at 1270 and 1358 cm^{-1} were assigned to -N (CH₂CH₂)₃ groups. The bands at 1471, 1403 and 1358 cm^{-1} were due to the stretching mode of -CH₃-C group attached with phenyl ring.

1.2. ¹HNMR Analysis

By observing Figure (2), the peak appeared at $\delta \approx 2.2$ for the -CH₂- groups attached to -O-ph ring while the peak appeared at $\delta \approx 4.3$ for -OH groups. The peak appeared at $\delta \approx 1.7$ for the -CH₃ groups; these peaks were shielded due to the effect of -CH-OH groups. The peaks appeared at $\delta \approx 3.4$ for -NCH₂ were shielded due to the attachment by -CH₂OH group. The peaks appeared as triplet at $\delta \approx 3.8$ for CH₂ were shielded due to the attachment to -Si-O group. The peaks appeared as doublet and triplet at $\delta \approx 6.8$ & 7.1 were assigned to phenyl -CH groups.

1.3. Gas Liquid Chromatography (GLC)

The GLC diagram for compound IV has been illustrated in Figure (3) in which the peak appeared at retention time 3.732 min and purity 44.075% was found to be diphenol diethylene ether. While the other peak appeared at retention time 16.7 min and purity 55.925% was the main product compound III.

1.4. Gel Permeation Chromatograph (GPC)

The GPC diagram for compound III was shown in Figure (4). The average molecular weight (M_w) was 444 and the polydispersity is unity. From these results, the main product has low molecular weight and the other product did not appear in GPC data. These data were matched with GLC

1.5. Elemental Analysis

The elemental analysis for compound III was recorded in Table (1).

Table (1): Elemental analysis for compound III

Parameter	Compound III	%
Molecular weight	455	
Formula	C ₂₀ H ₃₄ N ₂ O ₇ Si	
C%	Calculated	55.38
	Found	54.28
H%	Calculated	7.47
	Found	7.74
N%	Calculated	6.15
	Found	6.33
Si%	Calculated	6.37
	Found	6.35

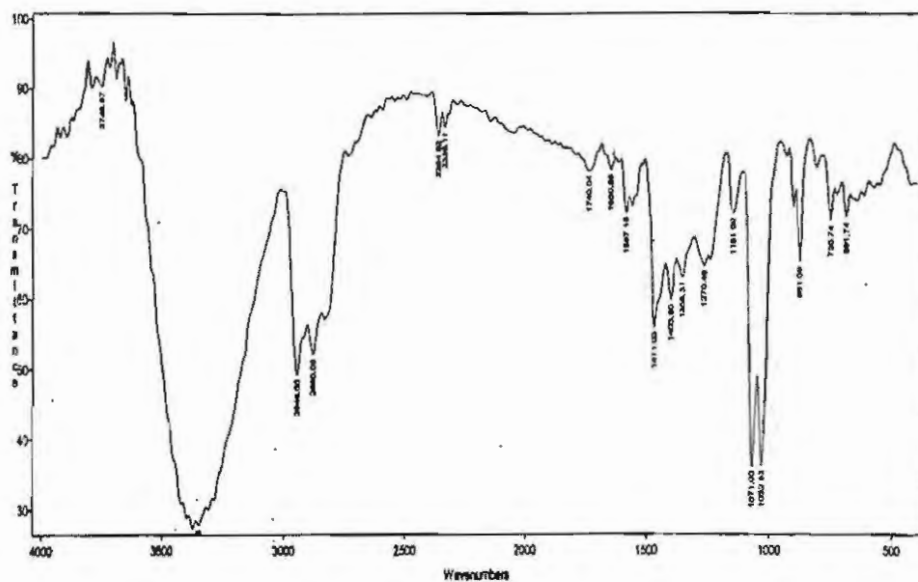


Fig. (1): FT-IR spectra of phenyl-ethanol di-triethanolamine siloxane (compound III)

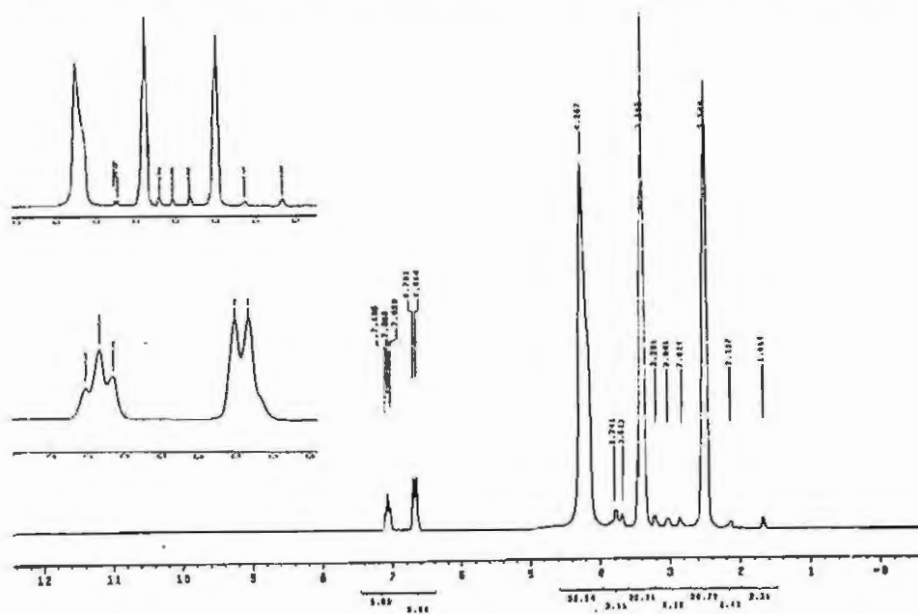


Fig. (2): ¹H-NMR for phenyl-ethanol di- triethanolamine siloxane (compound III)

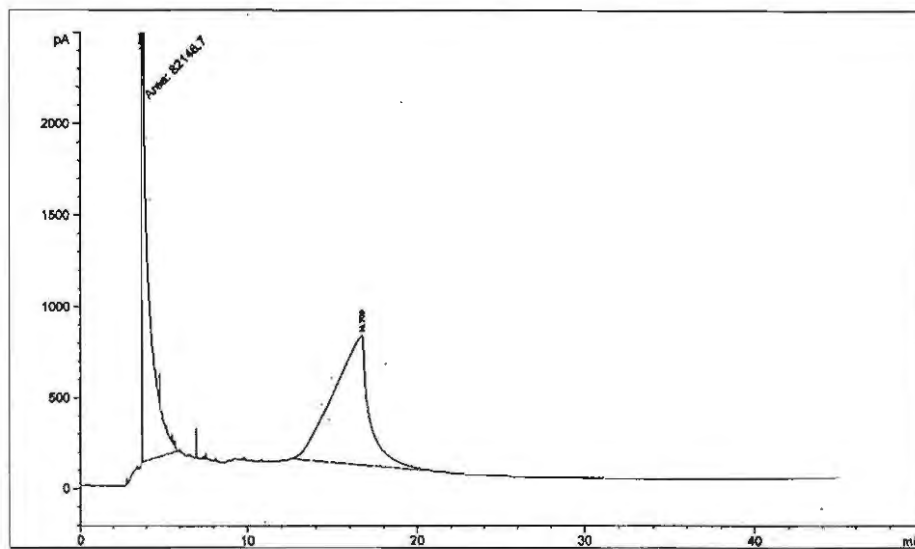


Fig.(3): Gas Liquid Chromatography for compound III

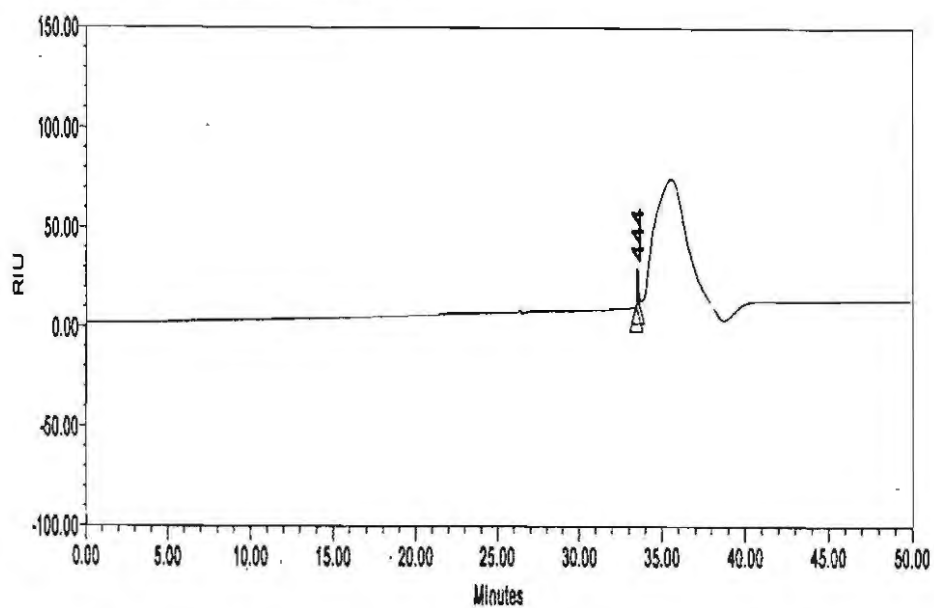


Fig. (4): Gel Permeation Chromatograph (GPC) for compound III

2. Physical and Mechanical Properties of the Formed Film on the Carbon Steel

Specimens :

2.1. Visual Inspection

Formulas (FA10-FA100) were applied at room temperature on the surface of carbon steel specimens by brushing and spraying methods. The formed films were visually inspected and noticed to be free from sealing, sagging, fish eyes, shrinking and coagulation. The formation films during and after curing on the surface of carbon steel specimens were appeared as one layer compatible with each other, compact and stable adhere as well as to the surface of carbon steel specimens which it was smooth and homogeneous.

2.2. Adhesion Forces of the Formed Dry Films

The adhesion forces data of the formed dry film using formulas (FA10-FA100) on the surface of carbon steel specimens were determined by X-cut tape and cross-cut tape techniques.

In all cases, the adhesion forces of the formed dry film were found to be excellent, and the rate of adhesion forces was 5A (No peeling or removal) and 5B (the edges of the cuts are completely smooth; none of the squares of the lattice is detached) depending on both two techniques X-cut tape and cross-cut tape respectively. Also, the resin compound and inorganic additives were found to contribute for increasing the adhesion forces between the surface of carbon steel specimens and the formed dry film as well as with itself.

2.3. Holiday (pinhole) Detection of the Formed Dry Films

The measuring voltages of pinhole for the formed dry films are depending on the dry film thickness of the formed films according to the following equation.

$$\text{Measuring voltages} = 5 \times \text{DFT} \dots\dots\dots (4)$$

The measuring voltages for the formed dry film were 400 ± 25 volts. The protection values were depending on the resin additive ratios and the inorganic filler, reflecting good compatibility of the fillers with the organic resin to form the poly urethane amide epoxy resin. These films were found to have good insulating properties. Therefore the formation dry films using formulas (FA10-FA100) are promising as insulator of the carbon steel surface. These films were free from discontinuity (void, crack, foreign inclusion, thin spot or contamination) in the coating film.

2.4. Thermal Cycling Test

The data of the thermal cycling test for the formed dry films using the formulas (FA10-FA100) were listed in Table (2). The temperature was ranged from 50 to 500 °C by increasing 50 °C in each interval. The formed dry films were affected by temperature in which the weight losses increased with increasing temperature, until 500 °C crevices have been taken place. From these results, the addition of compound III leads to the improvement of thermal stability of the formed dry films.

Table (2): Thermal cycling test of the formed dry films using formulas (FA10-FA100)

Temp. °C	Period Time.	Weight losses for each formed films $\times 10^{-4}$ gm									
		FA10	FA20	FA30	FA40	FA50	FA60	FA70	FA80	FA90	FA100
50		57	152	213	284	325	395	452	561	632	695
100		64	193	293	355	389	442	531	593	669	721
150		121	251	342	456	493	524	587	654	741	836
200		267	372	425	510	567	621	683	721	783	864
250	3hr s	315	394	462	546	593	652	712	755	842	912
300		387	425	562	610	657	698	717	789	885	956
350		467	543	625	654	692	731	794	843	932	987
400		536	586	672	732	786	813	854	897	947	1045
450		650	713	748	765	823	875	912	945	985	1167
500		Fail	Fail	Fail	Fail	Fail	Fail	Fail	Fail	Fail	Fail

2.5. Hardness Properties

It has been used to determine the cure of these coatings. Inspection of these data show a high values (9H) of the hardness which are stable with increasing the furan ratio. The formation dry film was cured completely after 5 days.

2.6. Impact Property

This test has been found to be useful in predicting the performance of organic coatings for their ability to resist cracking caused by impacts. From these data, the formed dry films were found to be free from any cracking and fixed on the surface of carbon steel specimen.

2.7. Bending Property

The bending property is an important mechanical test for evaluating the flexibility of coatings on the surface of the carbon steel specimens. This test has been determined by the resistance of dry films to cracking of the coating material. From these data, the dry films were found to be highly flexible.

3. Corrosion Studies:

3.1. Salt Spray Test

Salt spray test measures the ability of various types of coating to withstand the high corrosive (5% NaCl solution) medium.

Figure (5) illustrates the paint coated of the carbon steel specimen after exposure to salt spray fog for 21 days at 40 °C. Results indicate that the formed dry film using formulas (FA10-FA90) were free from any blister and cannot be removed in any direction from the areas surrounding the scribe edge with a pull by plastic tape. While a spot of little blister on the surface was noticed with the formed dry film using formula (FA100) after 12, 16 and 21 days which can be removed.

There are a little rust spots along the scribe areas on the formed dry film using formulas (FA10-FA90), which can be negligible, this rust was not remarkable over the dry film coated surface and was not spreading under these film. The results show that the rust at

scribe edge has no effect on the dry film coated in the presence of the quantity of compound III to furan resin in formulas (FA10-FA90). Compound III may improve the adhesion of the formed dry film on the specimen surface and prevent the spreading of it up and under film where, the compound III have high molecular weight and phenol ring, so that, it have more distribution, closed any voids in film surface, compacted and adhesion properties with specimen surface and component of film.

From all salt spray data, one can conclude that the coated surfaces containing compound III were highly corrosion resistant.

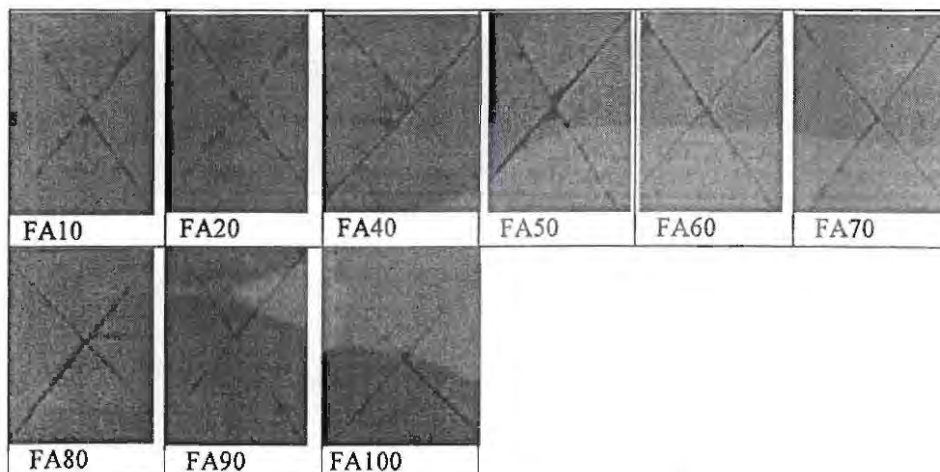


Figure (5): The surface texture of the formed dry films using (FA10- FA100) in case of salt spray test and after 21 days at 40 °C

3.2. Electrochemical Studies

The electrochemical studies are important to determine the validity of the formed dry film on the surface of carbon steel using formulas (FA10-FA100) as corrosion protection. Four types of electrochemical techniques were used namely: open circuit potential (OCP), potentiodynamic polarization, cyclicvoltametry (CV) and impedance (EIS). These studies were carried out in 3.5% NaCl solution as aggressive media. The experiments were conducted in cell contained coating carbon steel as working electrode, saturated calomel electrode as reference electrode and platinum wire as counter electrode.

3.2.1. Open Circuit Potential Measurements

The OCP values for the blank and formed dry films using formulas (FA10, FA20, FA40, FA50, FA60, FA70 and FA90) in 3.5% NaCl were -399,-566,-580,-625,-632,-650,-666 and -674 mV, respectively and shown in Figure (6). The blank specimen was pitted due to formation of ferrous hydroxide after 30 minutes and the curve jumped again at 50 minutes, i.e the corrosion phenomena was accelerated. The formed dry films were homogeneous and there is no any type of ferrous ions. These values decreased initially, then steady after 10 minutes then shifted towards negative direction after 30

minutes. So, the presence of compound (III) in the composition of formulas (FA) was able to protect the carbon steel surface against the corrosive medium (3.5% NaCl).

3.2.2. Potentiodynamic Polarization

The Tafel polarization curve obtained with the carbon steel blank and the formed dry films using formulas (FA10, FA20, FA40, FA50, FA60, FA70 and FA90) on the sample electrodes in 3.5% NaCl solution at voltage range from -1000 to -250 mV is depicted in Figure (7). The cathodic current for the blank increased, indicating a poor protection of the metallic substrate. The corrosion rate increased on the specimen surface due to the fact that NaCl solution contains different amount of water, oxygen, Na^+ , Cl^- and OH^- ions developed from the oxygen reduction as the main cathodic reaction. The reduction of iron compounds forming protective layer could be taking place together with oxygen reduction. It was deduced that the oxide layer formed on the electrode shown a certain protective ability. The anodic branch of the Tafel polarization curve revealed that carbon steel did not passivate in 3.5% NaCl. In case of the coated carbon steel, the polarization curves shifted from right to left and the corrosion currents decreased. Therefore, a higher corrosion inhibition due to the formation of dry films was obtained. It's obvious that the shift is only affecting the cathodic polarization curves, while no change in the anodic polarization curves. On the other hand, the formulas were highly efficient as cathodic and anodic protective materials. The corrosion potential (E_{corr}) and corrosion current density (i_{corr}) calculated automatically by using the Volta Lab PGZ 301 program have been given in Table (6) and it was evident from Figure (7) that E_{corr} shifts toward higher cathodic values at -666.8 mV versus SCE than uncoated carbon steel specimen. This shift was due to the presence of metallic zinc in the coating. The corrosion efficiency IE% and the surface coverage θ were calculated from the following equations [Deyab, M.A. (2007).]:

$$IE\% = \left(1 - \frac{i_{\text{coat}}}{i_{\text{uncoat}}}\right) \times 100 \dots\dots\dots (5)$$

$$\theta = \left(1 - \frac{i_{\text{coat}}}{i_{\text{uncoat}}}\right) \dots\dots\dots (6)$$

where i_{coat} and i_{uncoat} were the coated and uncoated current densities respectively. From Figure (7) and Table (3), IE% and surface coverage θ were found to decrease with increasing furan concentrations in the formulas under study. From polarization data, one can conclude that the coated surfaces containing compound (III) were highly efficient

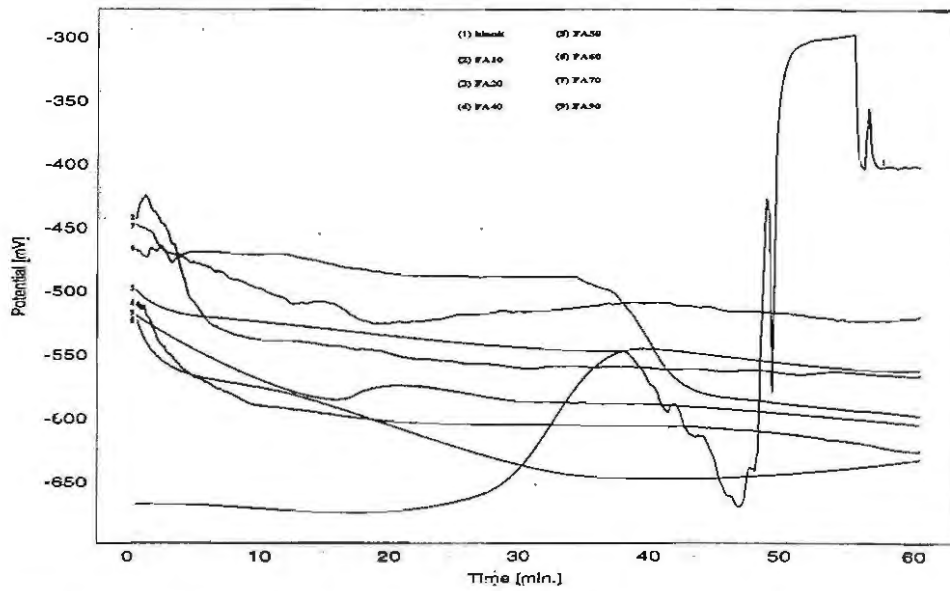


Fig.(6): The variation of Open Circuit Potential using blank and Formulas FA

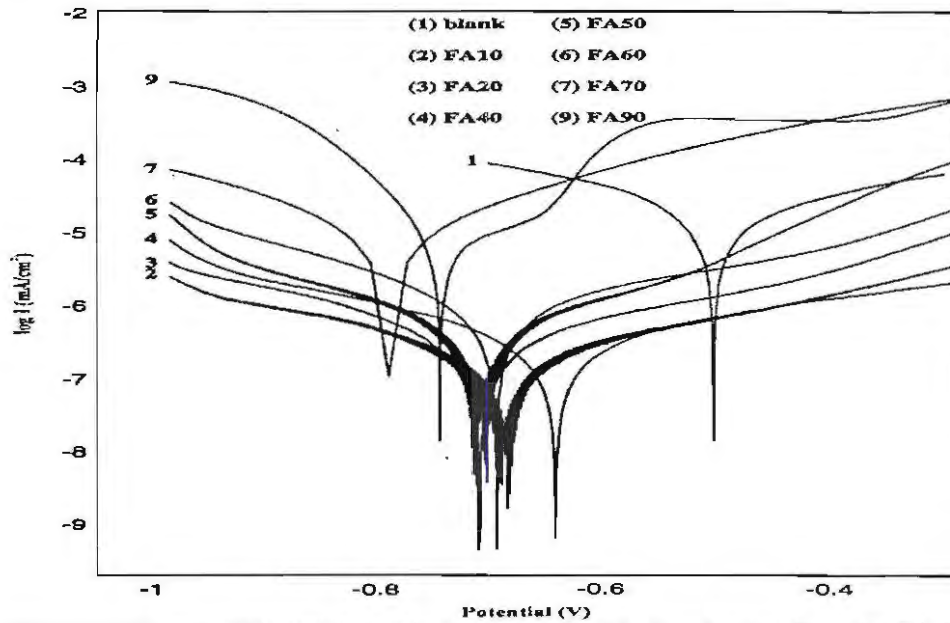


Fig.(7): Tafel potentiodynamic polarization curve for blank and using formulas FA in 3.5% of NaCl solution and potential range from -1.0 to -0.25 volt

Table (3): Potentiodynamic polarization parameters of formulas FA

Parameter Samples	$-E_{corr}$ (mV/SCE)	$I_{corr} \times 10^{-5}$ (mA/cm ²)	R_p (ohm cm ²)	ba (mV/dec)	-bc (mV/dec)	θ	IE%
Blank	518.80	2268	3562	436.90	329.70	-	-
FA10	789.30	2	1743051	188.50	140.60	0.999	99.90
FA20	726.60	4	1386666	312.30	216.00	0.998	99.80
FA40	760.30	9	631250	518.10	175.70	0.996	99.60
FA50	710.90	11	619020	442.80	243.50	0.995	99.50
FA60	657.60	17	418790	386.80	285.90	0.993	99.30
FA70	716.50	20	200655	288.50	136.60	0.99	99.00
FA90	738.50	28	145298	203.30	174.90	0.987	98.70

3.2.3. Cyclicvoltametry (CV)

The cyclic voltammetric behavior of carbon steel as blank and dry films formed using formulas FA was studied in the aqueous phase using 3.5% NaCl solution. The important parameters in a cyclic voltammogram are the peak potentials (E_{pc} , E_{pa}) and peak currents (i_{pc} , i_{pa}) of the cathodic and anodic peaks, respectively. A ratio between the peak current passed at reduction i_{pc} and peak passed at oxidation i_{pa} was near unity [Nicholson, R.S. *et al* (1964) Jurgen Heinze., (1984) and Perez, F. R. *et al* (2005).]

$$\frac{i_{pa}}{i_{pc}} = 1 \dots\dots\dots (7)$$

The voltage separation between the current peaks was

$$\Delta E = E_{pa} - E_{pc} = 2.303 \frac{RT}{nF} \dots\dots\dots (8)$$

where R universal gas constant (8.3144 J mol⁻¹k⁻¹), T absolute temperature (K), n number of electrons transferred, F = Faraday's constant (96,485 C/mol). Thus, for a reversible redox reaction at 25 °C with n electrons ΔE_p equal 0.0592/n V or about 0.60V for one electron [Nicholson, R.S. *et al* (1964) and Jurgen Heinze., (1984)].

The half cell potential $E_{1/2}$ can be determined using the following equation

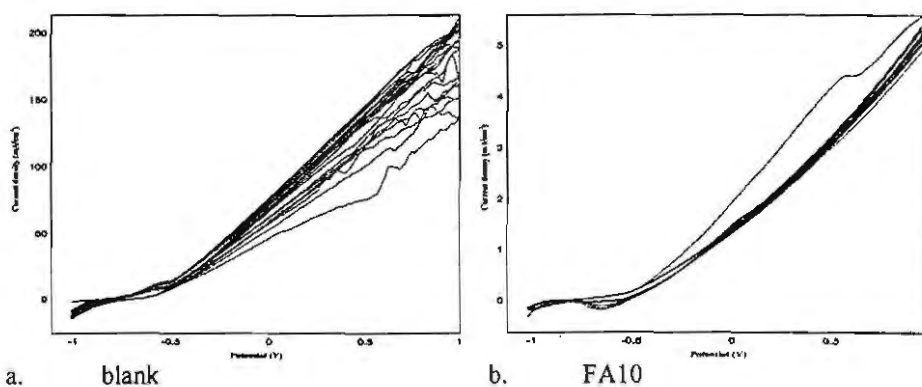
$$E_{\frac{1}{2}} = \frac{E_{pa} + E_{pc}}{2} \dots\dots\dots (9)$$

A single reversible redox process produces a pair of peaks of equal height centered on the reduction potential.

3.4.1. Carbon Steel Specimen (blank) in 3.5% NaCl Solution

Figure (8 (a-h)) shows the cyclic voltammograms obtained for carbon steel blank and coating carbon steel in 3.5 % NaCl solution for 10th cycles. It can be seen from this curve no change in cathodic area was observed in the cyclic voltammogram, while in the oxidation area from 0 mV to +1000 mV, the cycles were changed from each other at +500 to +1000 mV and there is some cavities formed due to pitting. One can conclude that the formation of ferrous ions at the cathodic area was reduced. The oxidation peak for FA10 was not appeared because there is no change and the cycles were identical in the anodic region. Two reduction peaks appeared for the formulas FA40, FA50, FA60 and FA90 in the forward and backward scans. The anodic peak potentials shift towards higher potentials while the cathodic peak potentials shift towards lower potentials, with

the scan cycles. Also, one can observe that the oxidation and reduction potentials are different. This fact was attributed to the electrostatic force in the form of an electrical double layer formed at the coating/surface interface. A furan, epoxy, novolac and compound III contains reactive hydroxyl groups that can react with toluene diisocyanate TDI to form polyurethane group. The increase in anodic current peak height and reduction in cathodic current peak height when the cycles scan repeat confirm the stability of the formed dry film. The peak-current ratio of the reverse and forward scans (i_{pa}/i_{pc}) was found to be very close to unity and independent of the cyclic scan. However, the anodic and cathodic peak separation (ΔE_p) for this wave was found to be higher than the expected theoretical ideal value (0.6 V for a one electron-transfer process) [Nicholson, R.S. *et al* (1964) and Jurgen Heinze, (1984)]. Large peak separation (ΔE_p) values can be obtained in the case of slow or quasi-reversible electron-transfer kinetics. The values of the ratio i_{pa}/i_{pc} were zero for formula FA10 but for the other formulas it was greater than unity and the values of the $E_{1/2}$ were small. From these values, the redox processes were found to be semi-reversible. In the reversible redox process, the transferred charge in the reduction and oxidation stages is the same and thus, their ratios equal unity; however, in formula FA10 with cyclic scan, this charge ratio was found to be less than unity because the oxidation current peak values were disappeared with increasing the cyclic scan. This may be due to the fact that reduction takes place at a lower current density than oxidation and it was not changed in the anodic region. But with respect to formulas FA20, FA40, FA50, FA60, FA70 and FA90, this charge ratio was greater than unity. This may be due to the fact that reduction takes place at a lower current density than oxidation and some oxidized materials may be adsorbed on the electrode's surface. From these data, one can observe that the formed dry films using the formulas under study were suitable for cathodic protection.



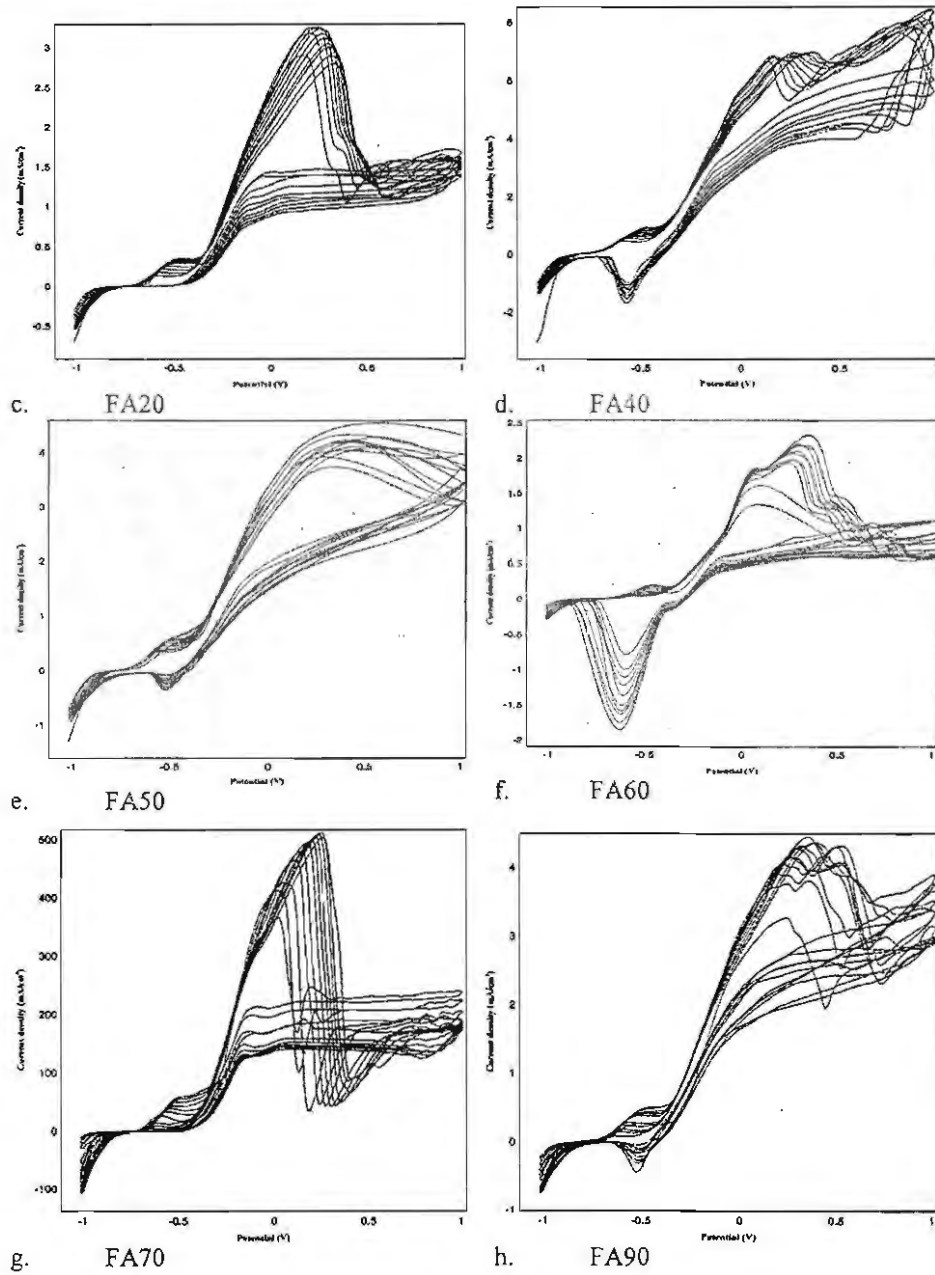


Fig.(8): Cyclic voltammogram curves for a: blank b: FA10 c: FA20 d: FA40 e: FA50 f: FA60 g: FA70 and h: FA90 of carbon steel specimen in 3.5% NaCl solution and potential range from -1.0 to +1.0 volt

Table (4): The parameters ΔE_{p-p} , $E_{1/2}$, E_{pa} , E_{pc} , i_{pa} , i_{pc} , i_{pa}/i_{pc} of the formulas FA10, FA20 and FA40

Parameters Scan No.	FA10			FA20			FA40					
	ΔE_p (V)	$E_{1/2}$ (V)	i_{pa}/i_{pc}	ΔE_p (V)	$E_{1/2}$ (V)	i_{pa}/i_{pc}	ΔE_{p1} (V)	ΔE_{p2} (V)	$E_{1/2}$ (V)	$E_{1/2}$ (V)	i_{pa}/i_{pc1}	i_{pa}/i_{pc2}
1 scan	0.55	0.27	0.00	0.56	0.10	26.00	0.67	0.74	0.10	0.12	50.00	10.00
2 scan	0.56	0.29	0.00	0.62	0.09	19.28	0.74	0.78	0.09	0.11	26.00	5.20
3 scan	0.57	0.30	0.00	0.73	0.05	15.55	0.76	0.82	0.08	0.11	18.00	4.90
4 scan	0.58	0.31	0.00	0.76	0.04	13.80	0.82	0.88	0.06	0.09	14.00	4.66
5 scan	0.59	0.32	0.00	0.79	0.04	13.33	0.87	0.92	0.04	0.06	11.60	4.14
6 scan	0.60	0.33	0.00	0.82	0.03	12.20	0.93	0.97	0.03	0.04	10.33	4.13
7 scan	0.62	0.34	0.00	0.85	0.03	11.16	0.98	1.02	0.02	0.01	9.14	3.76
8 scan	0.63	0.35	0.00	0.88	0.02	9.71	1.03	1.06	0.03	0.01	8.25	3.66
9 scan	0.64	0.36	0.00	0.92	0.02	9.07	1.06	1.09	0.04	0.03	7.55	3.57
10 scan	0.65	0.37	0.00	0.96	0.02	8.75	1.10	1.12	0.05	0.04	7.00	3.50

Table (5): The parameters ΔE_{p-p} , $E_{1/2}$, E_{pa} , E_{pc} , i_{pa} , i_{pc} , i_{pa}/i_{pc} of the formulas FA50 and FA60

Parameters Scan No.	OFA ^a						FA60					
	ΔE_{p-p1} (V)	ΔE_{p2} (V)	$E_{1/2}$ (V)	$E_{1/2}$ (V)	i_{pa}/i_{pc1}	i_{pa}/i_{pc2}	ΔE_{p1} (V)	ΔE_{p2} (V)	$E_{1/2}$ (V)	$E_{1/2}$ (V)	i_{pa}/i_{pc1}	i_{pa}/i_{pc2}
1 scan	0.60	0.70	0.10	0.15	7.60	38.00	0.62	0.82	0.09	0.19	140.00	3.50
2 scan	0.65	0.75	0.08	0.13	7.26	25.66	0.66	0.85	0.08	0.18	26.66	3.20
3 scan	0.68	0.78	0.07	0.12	7.09	19.50	0.69	0.87	0.08	0.17	18.00	2.25
4 scan	0.72	0.82	0.06	0.12	6.58	15.80	0.73	0.91	0.062	0.15	14.61	1.90
5 scan	0.76	0.86	0.05	0.09	6.25	13.33	0.76	0.93	0.06	0.14	13.00	1.50
6 scan	0.81	0.91	0.02	0.07	6.03	11.71	0.80	0.96	0.05	0.13	10.00	1.33
7 scan	0.83	0.93	0.02	0.06	6.00	10.50	0.83	0.98	0.05	0.12	10.00	1.50
8 scan	0.87	0.97	0.02	0.05	5.97	9.55	0.87	1.02	0.04	0.12	9.56	1.37
9 scan	0.91	1.01	0.02	0.04	5.78	9.16	0.90	1.04	0.03	0.10	9.58	1.35
10 scan	0.95	1.05	0.03	0.03	5.62	9.00	0.95	1.07	0.03	0.10	9.60	1.33

Table (6): The parameters ΔE_{p-p} , $E_{1/2}$, E_{pa} , E_{pc} , i_{pa} , i_{pc} , i_{pa}/i_{pc} of the formulas FA70 and FA90

Parameters Scan No.	FA70			FA90					
	ΔE_p (V)	$E_{1/2}$ (V)	i_{pa}/i_{pc}	ΔE_{p1} (V)	ΔE_{p2} (V)	$E_{1/2}$ (V)	$E_{1/2}$ (V)	i_{pa}/i_{pc1}	i_{pa}/i_{pc2}
1 scan	0.50	0.15	360.00	-0.63	0.68	0.09	0.11	30.00	30.00
2 scan	0.53	0.16	26.66	0.67	0.73	0.08	0.11	23.33	23.33
3 scan	0.56	0.14	20.50	0.72	0.79	0.06	0.01	19.00	19.00
4 scan	0.64	0.12	14.33	0.78	0.87	0.04	0.01	16.00	16.00
5 scan	0.67	0.12	11.25	0.82	0.92	0.03	0.08	13.66	13.66
6 scan	0.70	0.11	9.40	0.87	0.97	0.02	0.07	12.00	12.00
7 scan	0.72	0.11	8.00	0.90	1.00	0.01	0.06	10.75	10.75
8 scan	0.75	0.11	7.00	0.95	1.05	0.01	0.05	9.77	9.77
9 scan	0.78	0.10	6.25	0.98	1.08	0.01	0.04	9.00	9.00
10 scan	0.80	0.10	5.77	1.02	1.12	0.01	0.04	8.36	8.36

3.2.4. Electrochemical Impedance (EIS)

The Electrochemical impedance spectroscopy (EIS) has been used extensively as a tool for investigation the mechanisms involving passivity and localized corrosion studies. Also used for evaluating the properties of surface modified and coated materials by characterization the paint film on metal substrate through two phenomena: The deterioration of the organic coating caused by exposure to electrolyte and the increase in corrosion rate of the underlying substrate.

Figure (9) shows the component elements for equivalent circuit models of the uncoated and coated carbon steel specimen, in which R_s : electrolyte resistance [the resistance of the electrolyte between the reference electrode and working (coated carbon steel) electrode]; R_{pore} : pore resistance [the resistance of the coating change during exposure due to the penetration of electrolyte into the micropores of the coating]; $C_{coating}$: coating capacitance [the capacitance of the organic coating] which an important parameter to be measured during coating failure; since all these factors cause the impedance/frequency relationship to be non-linear, they were taken into consideration by replacing one or more capacitive components (Q) of the equivalent circuit transfer function by the corresponding constant phase element (CPE). R_p : polarization resistance [the corrosion rate of the metal substrate beneath the organic coating]. While the parameters R_{ct} : charge transfer and C_{dl} : double layer capacitance [an electrical double layer exists at the interface between the electrode and its surrounding electrolyte]; where the parameters R_{ct} and C_{dl} yield information on the corrosion process at the bottom of the pores in the coating.

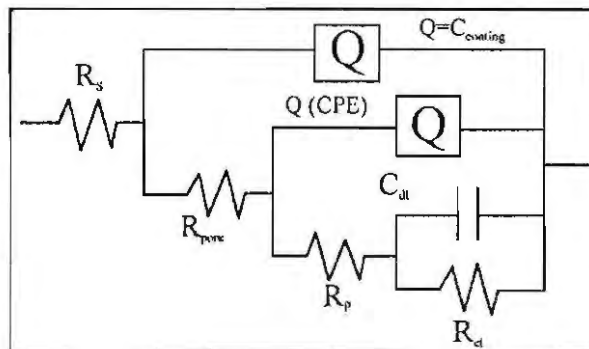


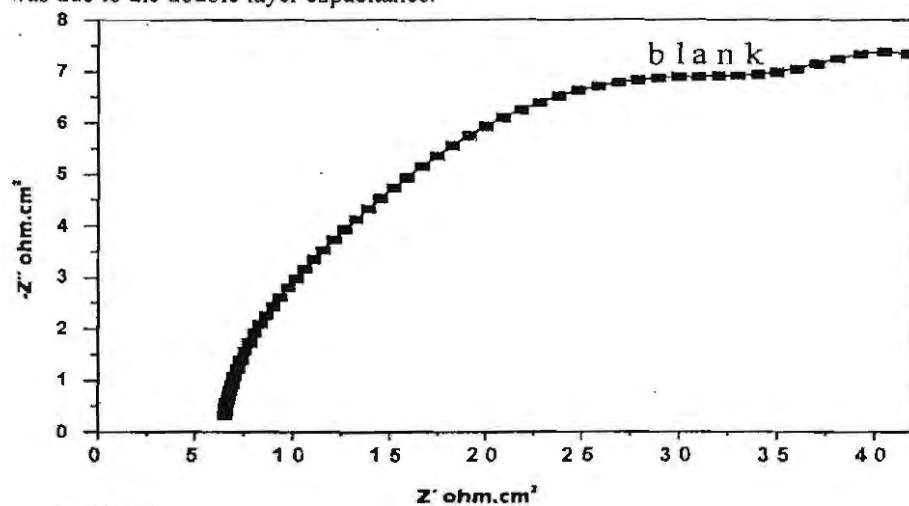
Figure (9): Equivalent circuit used for EIS calculations of formulas FA

3.2.4a. EIS Measurements for Carbon Steel Specimen (blank)

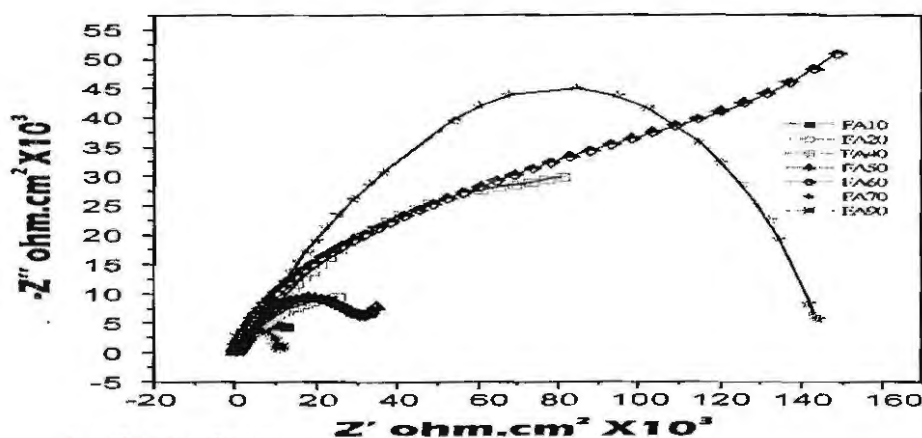
Inspection of Table (7) which shows EIS measurements of the blank reveals that R_s was very low and can be ignored; $C_{coating}$ indicates the beginning of constitution of the corrosion products on the substrate surface, R_{pore} was much decreased indicating the increase of porosity on the carbon steel surface. R_p was equal the standard value (5000 ohm-cm²) for carbon steel metal and the corrosion rate of the metal substrate described by polarization resistance. C_{dl} was less than the standard value (10⁻⁵ to 4x10⁻⁵ F/cm²) for carbon steel metal [David Loveday, *et al* (2004)]. Finally, the values of Q (CPE) and n indicate the heterogeneity of the oxide layer formed on the carbon steel specimen.

The Nyquist plot obtained for uncoated carbon steel electrode (blank) in 3.5% NaCl

solution has been given in Figure (10a). The feature of the curve was a slightly depressed semicircle, since there was not any coating on the electrode surface and a passivation could be expected to form under these conditions, the diameter of the curve must be equal to charge transfer resistance (R_{ct}) and the semicircle at lower frequency was due to the double layer capacitance.



a. blank



b. FA10 to FA90

Fig.(10): The Nyquist plot obtained for carbon steel specimen surface (blank) and dry film formation using FA10, FA20, FA40, FA50, FA60, FA70 and FA90 formulas in 3.5% NaCl solution

Studying Table (7) shows that R_s values were very low and can be canceled. $C_{coating}$ values were increased after immersion (1h) in the corrosive medium and the values of R_{pore} were decreased with increasing the furan ratio. It can be seen that minor difference was detected among the values corresponding to all of them, R_{pore} values were greater

than 10^{10} (ohm/cm^2) and the C_{coating} values were lower than 10^{-12} F/cm^2 confirm the excellent barrier properties afforded by the FA formulas and the paint film was in all cases able to keep the steel substrate isolated from the action of the corrosive electrolyte. It can be seen that low Q values, associated with the capacitance of the intact part of the coating film gives ($0.7 \leq n \leq 1$). Therefore, the magnitude of these two parameters also contributes to demonstrate that the paint coating actually behaved like a dielectric capacitor throughout the test. Figures (10b) show the Nyquist plots obtained for formulas FA10, FA20, FA40, FA50, FA60, FA70 and FA90 electrode in corrosive test solution. The diagrams consist of a linear portion at high frequencies and a depressed semicircle at lower frequency region for formula FA60 which was due to the double layer capacitance.

Table (7): EIS measurements in absence and presence of the formulas FA

Parameters Formula	R_s (ohm cm^2)	C_{coating} (F/cm^2)	R_{pore} (ohm cm^2)	$Q(\text{CPE})$ (F/cm^2)	n	R_p (ohmcm^2)	C_{dl} (F/cm^2)	R_{ct} (ohm cm^2)
Blank	6.43	1.8×10^{-5}	100	96×10^{-6}	0.37	4521	0.23	6.20
FA10	17.81	4.1×10^{-12}	9.1×10^{10}	1.4×10^{-9}	0.97	9.9×10^{12}	5.2×10^{-9}	8.4×10^{16}
FA20	15.95	5.3×10^{-12}	6.4×10^{10}	2.3×10^{-9}	0.97	4.6×10^{12}	9.4×10^{-9}	8.2×10^{16}
FA40	13.04	6.3×10^{-12}	5.3×10^{10}	2.5×10^{-9}	0.94	9.4×10^{12}	9.7×10^{-9}	7.8×10^{16}
FA50	10.09	6.8×10^{-12}	4.6×10^{10}	3.7×10^{-9}	0.89	3.5×10^{12}	10.4×10^{-9}	6.3×10^{16}
FA60	8.55	7.7×10^{-12}	4.1×10^{10}	4.2×10^{-9}	0.81	3.4×10^{12}	13.0×10^{-9}	5.9×10^{16}
FA70	7.36	8.1×10^{-12}	2.1×10^{10}	5.0×10^{-9}	0.79	8.3×10^{10}	13.7×10^{-9}	4.2×10^{14}
FA90	6.89	9.2×10^{-12}	1.0×10^{10}	8.4×10^{-9}	0.78	2.1×10^{10}	14.2×10^{-9}	2.3×10^{13}

4. Surface Morphology of Dry Films before and after EIS Measurements using SEM:

Figure (11a) shows the surface morphology structure of the dry film using formula FA90 as an example before EIS measurements. The lattice of the polymer resins was appeared as the surface cross-linkage, and so the inorganic filler and pigment materials were manifested as crystal and pseudo-crystal. These materials were emerged homogeneous distribution. Figure (11) illustrates the structure of the dry film using formula FA90 after EIS measurements. The interlock white lines found on the surface indicate that the network formation from crosslinkage between the hydroxyl, amine, epoxy and cyanate groups from the resin compounds. The weak white lines were due to the penetration of electrolyte into the micropores of the surface coating. The presence of zinc dust in the pigment modified the structure of the protective layer. Also, the samples were found to be free from blisters in the surface films. Generally, the morphology of the surface using FA formulas was different with few small defects even in the case of maximum deformation. This inspection confirms the results obtained from salt spray, open circuit, potentiodynamic polarization, cyclic voltametry and impedance.

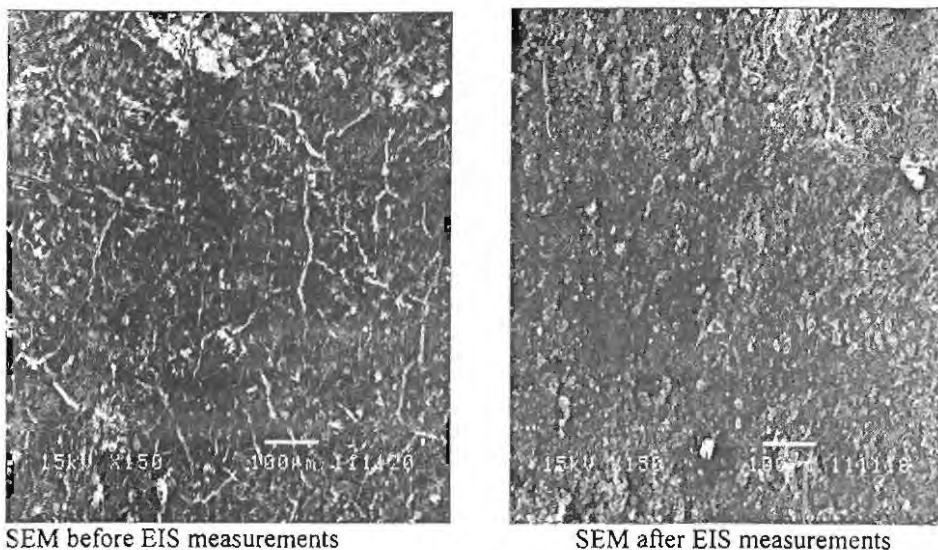
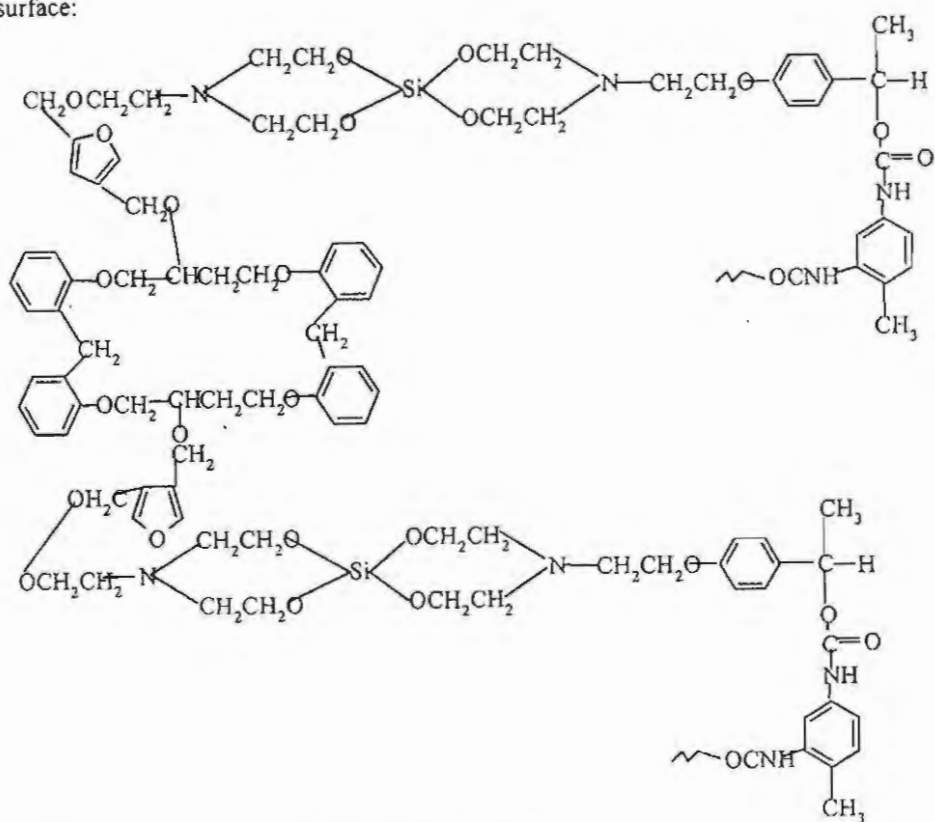


Figure (11): SEM micrographs at x150 magnifications using FA90 a: before EIS measurements and b: after EIS measurements

5. General Mechanism:

The chemical structure of the formed resin furan, epoxy, novolac, and organosilicon compounds including different active groups as hydroxyl and epoxide (oxiranes) groups. The epoxide or oxirane group has many useful reactions in resin chemistry to form polyether structure, which has an advantage because no volatiles were released during cure. Also the hydroxyl groups of furan and organosilicon compounds were reacted with oxirane groups to form ether groups. The polyhydroxyl groups were produced on the backbone chain (secondary hydroxyl group). The formation of hydroxyl groups were reacted (cured) with cyanate groups of TDI to form polyurethane melamine epoxy furan film. Also, some hydroxyl groups on the surface of silica were cured with some cyanate groups of TDI. These interactions gave a high molecular weight, stable, compact, adhesion and excellent improving lattice for the formed dry films. The inorganic pigment and filler had the following properties weather stability, surface hardness, flexibility, corrosion prevention, electrical resistance and adhesion for the films formed on the surface of carbon steel. The silicone-polyurethane chemistry allows the additives to migrate to the coating / substance interface thus providing wetting. By incorporating into additive coatings hydrophobic solids particular such as, titanium oxide, Zn dust, talc, CaCO_3 and sintered glass, effective foam control, filler / pigment. The silicon will control the formation of the foams because of their excellent compatibility; these products have a low tendency to cause defects for the coating. Thus the formed polyurethane films include the variation of very important groups, such as siloxane, urethanes and amide groups. So that these groups played an important role for the improvement of the physical, mechanical, thermal stability and chemical properties of the formed dry films on the surface of carbon steel. Finally, we can suggest the following scheme to explain the expected reactions taking place on the carbon steel

surface:



Scheme I: Formation lattice films using formula FA

CONCLUSIONS

1. Novel organosilicon compound was prepared and confirmed by: FT-IR, ¹HNMR, GLC, GPC and elemental analysis.
2. These compound was blended with furan, epoxy and novolac resin compounds
3. The blended compounds were formulated with Zn, TiO₂, CaCO₃ and talc as filler and pigment in different formulas (FA10-FA100) and the TDI were used as curing agent.
4. The effect of physical, mechanical and chemical environment was studied to show the resistivity of the formed films on the carbon steel against these parameters.
5. The hardness, impact and bending resistance values using the formulas under investigation were found to be stable with increasing the furan ratio in presence of the organosilicon compounds.
6. The results of: open circuit, potentiodynamic polarization, cyclic voltametry and impedance measurements indicated that the formed dry films by the formulas under investigation acted as cathodic inhibitors.
7. The results obtained from various techniques showed a good agreement with each other.

ACKNOWLEDGEMENTS

The authors wish to acknowledge the financial supports of the Egyptian Petroleum Research Institute (EPRI), Ahmed El-Zomor St., 1, Nasr City 11727, Cairo, Egypt and Chemistry Department, Faculty of Science, Al- Azhar University; Nasr City, Cairo, Egypt.

REFERENCES

- Attar, M.M. Mahdavian, M. A., Investigation on zinc phosphate effectiveness at different pigment volume concentrations via electrochemical impedance spectroscopy, *Electrochim. Acta* 50 (2005) 4645.
- Ashirgade, A. A. Seth, W.J. van Ooij, P. Puomi, Z. Yin, S. Bafna, C. Shivane, Novel, one-step, chromate-free coatings containing anticorrosion pigments for metals—An overview and mechanistic study, *Prog. Org. Coat.* 58 (2007) 136.
- Aronhime, M.T. Gillham, J.K. Effect of time-temperature path of cure on the water absorption of high Tg epoxy resins, *J. Appl. Poly. Sci.* 32 (1986) 3589–3626.
- Benbachir, A. Guenbour, A. Kacemi, A. Evaluation of the corrosion performance of zinc-phosphate-painted carbon steel, *Surf. Coat. Technol.* 113 (1999) 36.
- Blustein, G. Deya, M.C. Romagnoli, R. Del Amo, B. The influence of the anion type on the anticorrosive behaviour of inorganic phosphates, *Surf. Coat. Technol.* 150 (2002) 133.
- Bethencourt, M. F Botana, J. Marcos, M. Osuna, R.M. Sanchez-Amaya, J.M. Inhibitor properties of “green” pigments for paints, *Prog. Org. Coat.* 46 (2003) 280.
- Chromy, L. Kaminska, E. Non-toxic anticorrosive pigments, *Prog. Org. Coat.* 18 (1990) 319.
- Cabanelas, J.C. Serrano, B. Gonzalez-Benito, J. Bravo, J. Baselga, J. Morphology of epoxy/ polyorganosiloxane reactive blends, *Macromolecular Rapid Communications* 22 (2001) 694–699.
- Cabanelas, J.C. Prolongo, S.G. Serrano, B. Bravo, J. Baselga, J. Water absorption in polyaminosiloxane-epoxy thermosetting polymers, *Journal of Materials Processing Technology* 143–144 (2003) 311–315.
- Deyab, M.A. *Corros. Sci.*, 49, [2007] 2315-2328.
- David Loveday, Pete Peterson, and, Bob Rodgers, Evaluation of Organic Coatings with Electrochemical Impedance Spectroscopy, *JCT Coat. Technol.*, [2004] 88-93.
- Gnot, W. Zubielewicz, M. Mechanisms of non-toxic anticorrosive pigments in organic waterborne coatings, *Prog. Org. Coat.* 49 (2004) 358.
- Goulding, T.M. an Epoxy resins adhesiveso, in: A. Pizzi, K.L. Mittal (Eds.), *Handbook of Adhesive Technology*, Marcel Dekker, New York, (1994) 531.
- Gonzalez, M. Kadleca, P. Strachota A., Matejka, L. Crosslinking of epoxy-polysiloxane system by reactive blending, *Polymer* 45 (2004) 5533–5541.

Gonzalez, S. Mirza Rosca, I.C. Souto, R.M. Investigation of the corrosion resistance characteristics of pigments in alkyd coatings on steel, *Prog. Org. Coat.* 43 (2001) 282.

Jurgen Heinze, "Cyclic Voltammetry, Electrochemical Spectroscopy, New Analytical Methods". *Angewandte Chemie*, 11, (1984) 831-847.

Lezzi, R.A. Fluoropolymer coatings for architectural applications in modern fluoropolymers, John Wiley & Sons, Chichester, UK, (1997). 4274

May, C.A. *an Epoxy Resins; Chemistry and Technology*, Marcel Dekker, New York, (1988).

McIntyre, J.M. Pham, H.Q. Electrochemical impedance spectroscopy; a tool for organic coatings optimizations, *Prog. Org. Coat.* 27 (1996) 201.

Marchebois, H. Joiret, S. Savall, C. Bernard, J. Touzain, S. Characterization of zinc-rich powder coatings by EIS and Raman spectroscopy, *Surf. Coat. Technol.* 157 (2002) 151.

Nunes S.P., Schultz J, Peinemann KV. Silicone membranes with silica nanoparticles. *J. Mater Sci. Lett.*, 15 (1996) 1139-41.

Nunez, L. Villanueva, M. Fraga, F. Nunez, M.R. Nunez MR, Influence of water absorption on the mechanical properties of a DGEBA (n = 0)/1, 2 DCH epoxy system, *J. Appl. Poly. Sci.* 74 (1999) 353-358.

Nicholson, R.S.; Shain, I.; "Theory of Stationary Electrode Polarography. Single Scan and Cyclic Methods Applied to Reversible, Irreversible, and Kinetic Systems." *Anal. Chem.*, 36, (1964) 706-723,.

Pellice SA, Williams RJJ, Sobrados I, Sanz J, Castro Y, Aparicio M, Solutions of hybrid silica microgels as precursors of sol-gel coatings. *J Mater Chem* 16 (2006) 18-25.

Perez, F. R. Basáez, L. Belmar J. and Vanysek P. Cyclic Voltammetry, *J. Chil. Chem. Soc.*, 50, (2005) 575-580,.

Sinko, J. Challenges of chromate inhibitor pigments replacement in organic coatings, *Prog. Org. Coat.* 42 (2001) 267.

Shon, M. Kwon H., *Corros. Sci.* 49 (2007) 4259-4275

Xiao, G.Z. Shanahan, M.E.R. Irreversible interactions between water and DGEBA/DDA epoxy resin during hygrothermal aging, *J. Appl. Poly. Sci.* 65 (1997) 449-458.

Yeh JM, Weng CJ, Liao WJ, Mau YW. Anticorrosively enhanced PMMA-SiO₂ hybrid

coatings prepared from the sol-gel approach with MSMA as the coupling agent. Surf Coat Tech 17 (2006) 88-95.

Zhou, J.M. Lucas, J.P. Hygrothermal effects of epoxy resin. Part I: the nature of water in epoxy, Polymer 40 (1999) 5505-5512.

Zhang, J.T. Hu, J.M. Zhang, J.Q. Cao, C.N. Studies of water transport behavior and impedance models of epoxy-coated metals in NaCl solution by EIS, Prog. Org. Coat. 51 (2004) 145.

الملخص العربي

دور مركب فينيل- ايثانول ثنائي - ثلاثي ايثانول أمين سيلوكزان المحضر في تكوين غطّات البولي يوريثان لحماية الحديد الكربوني

اسامه محمود ابو العينين¹، محمد احمد عباس¹، ماهر عباس السكري¹ و حسن محمد

عبدالباري^{2*}

¹معهد بحوث البترول- اشرع احمد الزمر- مدينة نصر- القاهرة - مصر

^{2*} قسم الكيمياء- كلية العلوم بنين- جامعة الأزهر- مدينة نصر - القاهرة- مصر

تم تحضير مركب فينيل- ايثانول ثنائي - ثلاثي ايثانول أمين سيلوكزان

و التأكد من التركيب الكيميائي له باستخدام التقنيات الآتية :

طيف الأشعة تحت الحمراء- طيف الرنين النووي المغناطيسي- كروماتوجرافيا الغاز -

كروماتوجرافيا النفاذية الهلامية- تحليل العناصر

واستخدمت هذه المركبات في عمل تركيبات مختلفة تستخدم في دهانات أسطح الصلب

الكربوني محل الدراسة ، هذه التركيبات تحتوي على نسب مختلفة من الفيوران ونسبة ثابتة

من الإيبوكسي والنوفولاك والمواد العضو-سليكونية مع نسبة ثابتة من كل من الزنك وثاني

اكسيد التيتانيوم وكربونات الكالسيوم وبودرة التلك والزجاج الملبد كمخضبات / مالئة ونسبة

ثابتة من المذيب العضوي ميثيل ايثيل كيتون. وقد أستخدمت نسب مختلفة من ماده الطولوين

داى ايزو سيانيد كمادة (مصلدة) تساعد على سرعة الجفاف.

وقد تم تقييم الأفلام المتكونة قبل و بعد الجفاف بواسطة إجراء الاختبارات التالية:

- الفحص البصرى للأفلام المتكونة.
 - تعيين الخواص الفيزيائية
 - تعيين الخواص الميكانيكية
 - تقييم صلاحية الأفلام الجافة المتكونة بواسطة اختبارات التآكل وهي دراسة تأثير ماء البحر
 - الخواص الكهروكيميائية للأفلام المتكونة
 - فحص التركيب البلورى السطحى(المسح الالكترونى) قبل وبعد هذه الإختبارات.
- وبصفة عامة فإن نتائج هذه الإختبارات على الأفلام المتكونة بينت أن هذه الافلام ذات قدرة عالية على حماية أسطح الصلب الكربونى من التآكل تحت الظروف المختلفة وخاصة فى الحماية الكاثودية وكذلك ارتفاع كفاءتها وقلة تكلفتها الاقتصادية.